MBZUAI
Digital.Commons@MBZUAI

Computer Vision Faculty Publications | Scholarly Works

4-22-2022

Self-Supervised Video Object Segmentation via Cutout Prediction and Tagging

Jyoti Kini
University of Central Florida, United States

Fahad Shahbaz Khan
Mohamed bin Zayed University of Artificial Intelligence & Linköping University, Sweden

Salman Khan
Mohamed bin Zayed University of Artificial Intelligence

Mubarak Shah
University of Central Florida, United States

Follow this and additional works at: https://dclibrary.mbzuai.ac.ae/cvfp

 Part of the Artificial Intelligence and Robotics Commons

Preprint: arXiv
Archived with thanks to arXiv
Preprint License: CC by NC SA 4.0
Uploaded 24 May 2022

Recommended Citation

J. Kini, F.S. Khan, S. Khan, and M. Shah, "Self-Supervised Video Object Segmentation via Cutout Prediction and Tagging", arXiv, Apr 2022, doi: 10.48550/arXiv.2204.10846

This Article is brought to you for free and open access by the Scholarly Works at Digital.Commons@MBZUAI. It has been accepted for inclusion in Computer Vision Faculty Publications by an authorized administrator of Digital.Commons@MBZUAI. For more information, please contact libraryservices@mbzuai.ac.ae.

arXiv:2204.10846v1 [cs.CV] 22 Apr 2022

Self-Supervised Video Object Segmentation via Cutout Prediction and Tagging

Jyoti Kini
jyoti.kini@knights.ucf.edu
University of Central Florida
USA

Fahad Shahbaz Khan
fahad.khan@liu.se
MBZ University of Artificial Intelligence[1]
Linköping University[2]
UAE[1], Sweden[2]

Salman Khan
salman.khan@mbzuai.ac.ae
MBZ University of Artificial Intelligence
UAE

Mubarak Shah
shah@crcv.ucf.edu
University of Central Florida
USA

ABSTRACT

We propose a novel self-supervised Video Object Segmentation (VOS) approach that strives to achieve better object-background discriminability for accurate object segmentation. Distinct from previous self-supervised VOS methods, our approach is based on a discriminative learning loss formulation that takes into account both object and background information to ensure object-background discriminability, rather than using only object appearance. The discriminative learning loss comprises cutout-based reconstruction (cutout region represents part of a frame, whose pixels are replaced with some constant values) and tag prediction loss terms. The cutout-based reconstruction term utilizes a simple cutout scheme to learn the pixel-wise correspondence between the current and previous frames in order to reconstruct the original current frame with added cutout region in it. The introduced cutout patch guides the model to focus as much on the significant features of the object of interest as the less significant ones, thereby implicitly equipping the model to address occlusion-based scenarios. Next, the tag prediction term encourages object-background separability by grouping tags of all pixels in the cutout region that are similar, while separating them from the tags of the rest of the reconstructed frame pixels. Additionally, we introduce a zoom-in scheme that addresses the problem of small object segmentation by capturing fine structural information at multiple scales. Our proposed approach, termed CT-VOS, achieves state-of-the-art results on two challenging benchmarks: DAVIS-2017 and Youtube-VOS. A detailed ablation showcases the importance of the proposed loss formulation to effectively capture object-background discriminability and the impact of our zoom-in scheme to accurately segment small-sized objects.

KEYWORDS

self-supervision, video object segmentation, cutout, tagging, pretext tasks, attention

1 INTRODUCTION

Video object segmentation (VOS) aims to segment an object of interest in a video, given its segmentation mask in the first frame. VOS plays an important role in numerous real-world applications, such as interactive video editing, autonomous driving, augmented-reality, and smart surveillance systems. The problem is challenging since the target object is only provided with a reference segmentation in the first frame, and determining the object segmentation mask in all other frames involves: **a.** accounting for drastic changes in the appearance of the object of interest, over time, due to occlusion, **b.** distinguishing the object from highly similar surrounding distractor elements, and **c.** estimating finer object details, especially in case of a small object or object diminishing in size across the video sequence.

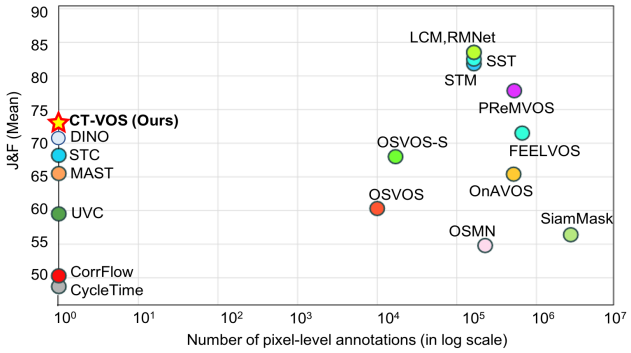

Figure 1: Comparison in terms of overall accuracy $J\&F(Mean)$ and pixel-level annotations required for different VOS methods on DAVIS-2017. The proposed CT-VOS outperforms existing self-supervised VOS methods. Different VOS methods shown here in comparison are: DINO [3], STC [17], MAST [21], UVC [24], CorrFlow [22], CycleTime [51], LCM [16], RMNet [53], SST [10], STM [33], PReMVOS [27], FEELVOS [44], OSVOS_S [28], OnAVOS [46], OSVOS [2], SiamMask [50], OSMN [57].

Most existing VOS approaches [4, 9, 33, 34, 42, 45, 54] typically rely on extensive supervision during training in the form of ground-truth human annotations (see Figure 1). Specifically, a common strategy is to fine-tune a network backbone, conventionally pre-trained on ImageNet [5], using additional data (*e.g.* MS COCO [26], Pascal VOC [11], DAVIS [35], YouTube-VOS [55]) with pixel-level supervision in the form of segmentation masks. Different from

these supervised approaches, recent self-supervised VOS methods [21, 22, 48, 51, 56, 60] perform segmentation without utilizing additional supervised training in the form of pixel-level ground-truth annotations. Several of these self-supervised approaches learn pixel-wise correspondence between frames by reducing the reconstruction error [21, 48], whereas others focus on matching pixels across frames using inherent cyclic consistency in videos [22, 51]. While promising results have been achieved by these self-supervised approaches, the performance still remains far from their supervised counterparts.

Typically, self-supervised VOS [21] approach employs robust pixel matching strategies to learn prominent representations of the target region while paying minimal focus on learning the feature embedding of the background region. Our methodology, however, is based on introducing feature diversity by taking into account both object and background information for object-background discriminability. The proposed cutout and tagging learning scheme encourages the object prediction model to focus on both prominent and non-prominent features of the target object as well as the background appearance, providing superior discriminative abilities. In addition, we alleviate a common problem encountered in several existing VOS methodologies that of loss of details, especially in small objects.

We introduce a self-supervised VOS approach, CT-VOS, that predicts the segmentation mask for the current frame based on the information in previous frames. Instead of learning trivial solutions from standard self-supervised color-based reconstruction loss between the current frame and previous frames, we utilize a two-fold discriminative learning loss formulation. *First,* instead of simply reconstructing the current frame, we also predict cutout in the current frame based on cutout in previous frames. Here, cutout represents a part of an image, whose pixels are replaced with some constant values *e.g.*, zero. Intuitively, cutouts effectively simulate occlusion-based discontinuities and thereby aid the model to deal with occlusions during inference. *Second,* the model predicts tags in the current frame, such that the tags of all pixels in the cutout region are similar, and also considerably different from tags of non-cutout pixels. Here, we generate a heatmap of per-pixel identity tags for the current frame, where each tag could be any arbitrary value between 0 and 1. Our tagging loss enables separating the cutout pixels from the reconstructed image pixels, thereby improving the VOS performance by mimicking foreground-background separation. These complementary formulations are designed to allow the model to learn a rich representation, rather than learning a trivial solution of assigning the exact same color to pixels. Furthermore, we utilize zoom-in views of a random frame that facilitates the model to deal with objects at different scales. To summarize, our contribution is multifold:

- We present an object-background discriminative loss formulation comprising a cutout-based reconstruction element and tagging loss component. While cutout-based reconstruction forces the model to focus on both salient as well as less salient aspects of the object of interest by simulating controlled spatio-temporal occlusion-based discontinuities, tagging loss effectively separates the object of interest from the background pixels by mimicking foreground-background separation.
- We introduce zoom-in views in our VOS architecture that enables processing small spatial regions and thereby captures fine-grained object details. The zoom-in scheme not only assists with tracking smaller objects but also improves the segmentation mask details generated for larger objects.
- Comprehensive qualitative and quantitative experiments are performed on two challenging benchmarks: DAVIS-2017 [35] and Youtube-VOS [55]. Our results reveal the benefits of object-background discriminative loss formulation and zoom-in scheme, outperforming all published self-supervised VOS methods on both benchmarks.

2 RELATED WORK

Hand-crafted features based on appearance, motion, spatial proximity, and neighbourhood grouping constraints have been used in earlier works [1, 12, 18, 30] on VOS. The need for extensive manual annotations in a supervised setting has encouraged researchers to venture beyond the supervised paradigm into the realm of self-supervised VOS. Based on the nature of supervision, existing VOS approaches can be roughly categorised into following three groups:

Supervised VOS Methods: A considerable volume of work on video object segmentation (VOS) task [4, 9, 33, 45, 54] focuses on segmenting each object instance separately. Several recent works [9, 42, 54], employ sequential modelling to achieve temporal consistency. Lately, a number of solutions have been motivated by embedding based approaches [34, 45], which deal with learning pixel-mappings between reference and target frames. One such prior work by Oh et al. [33], deals with binary-classification of each pixel to generate a single-object segmentation mask for a given frame by applying non-local matching with previously predicted frames. Another idea of the region based segmentation approach is used to extract multiple object proposals in a single feed forward-path, followed by associating objects across frames [23, 27]. However, the dependence of these approaches on region proposal networks [14, 38] and ground-truth annotations introduces additional complexities.

Few-Shot Learning Based Segmentation: Few-shot segmentation deals with learning to segment objects based on a limited set of annotated examples. Initial literature [7, 40, 41, 58] in this area focused on using labeled segmentation masks for few examples in the support set. Some of the latest methods [36, 49, 59] have worked with weaker annotations based on scribble or bounding boxes. Raza et al. [37] recently proposed using image-level labels to solve the supervision requirement in a few-shot segmentation task. Although this is a promising direction, these formulations are labor-intensive, especially in robotic applications that require learning online.

Self-supervised Segmentation: Self-supervised methods enable models to learn without manually generated supervisory signals, thereby eliminating the overhead of large annotated datasets. Generally, computer vision pipelines that employ self-supervised learning employ two tasks: a pretext task and a downstream task. Although the downstream task is the ultimate goal, the pretext task is the primary task that the self-supervised method seeks to solve. In the

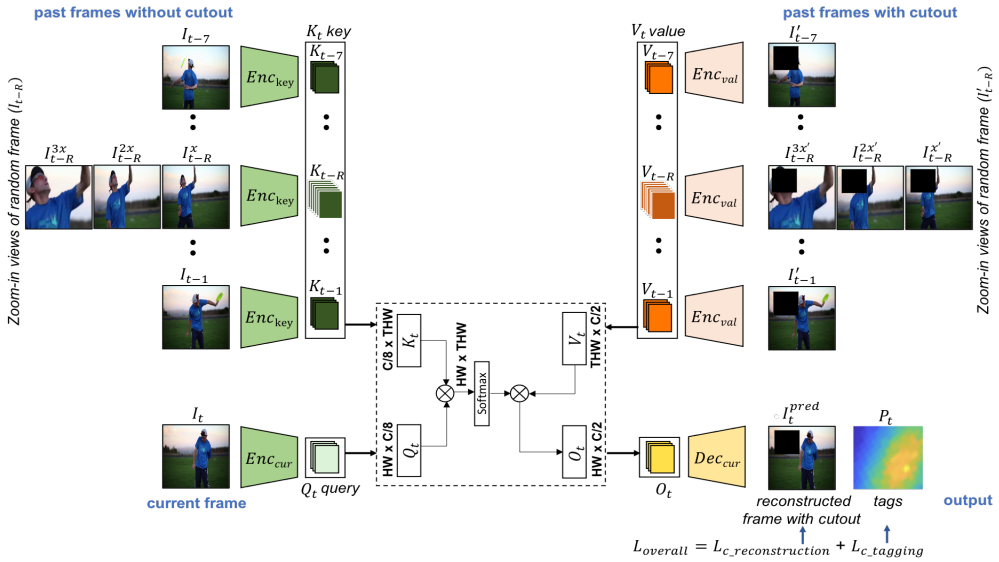

Figure 2: Overview of the proposed CT-VOS training. Firstly, the current frame I_t is used to generate query Q_t, and the past frames I_{t-1},…, I_{t-7} are employed to compute a comprehensive key set K_t (shown on the left). Next, the past frames with cutout I'_{t-1},…, I'_{t-7} are processed to yield the value set V_t (shown on the right). Then, the generated query, key and value are employed to predict the reconstructed frame with cutout I_t^{pred} and tag channel P_t (shown on the bottom right). In order to learn finer object details, we introduce zoom-based strategy by choosing a random frame I_{t-R} (shown on the left). Here, we introduce 3 different zoom levels in a chosen random frame. Therefore, with these three frames, the total number of frames, T, corresponds to 10 frames. $\otimes$ implies dot product.

literature, some pretext tasks have been explored to learn spatial context from images and videos [6, 21], while others have relied on the temporal ordering and consistency [19]. Generation of pseudo classification labels [20], future representations prediction [13, 47], jigsaw puzzles prediction [31], arrow of time [52] and shuffled frames [29] are some other popular pretext tasks. Recent work by Han et al. [13] uses contrastive learning on videos to learn strong video representations. In CT-VOS, instead of learning trivial solutions from standard self-supervised color-based reconstruction loss between the current frame and previous frames, we employ two-fold object-background discriminative loss formulation and a zoom-in scheme for self-supervision.

3 APPROACH

Given the first frame segmentation mask of an object, the proposed network segments the object throughout the video clip based on the context provided by the previous frames. Figure 2 illustrates the overall network architecture. We exploit the automatically available supervisory signals from data by framing VOS as a self-supervised learning problem. To this end, we introduce object-background discriminative loss formulation comprising cutout-based reconstruction and tag (cutout vs. non-cutout) prediction. While one of the components helps mimic occlusion-based spatio-temporal discontinues, the other encourages the model to generate well-separated foreground-background segmentation masks. We also utilize zoom-in views of a random frame that enriches the overall representation by capturing the segmentation details at different scales.

Initially, the current frame is processed through an encoder setup to generate *current frame embedding - query* (Figure 2). Next, previous frames are encoded to *past frame embeddings - keys*. The query interacts with keys to generate similarities between the current and previous frame content. Then, the *values* are extracted using previous frames with introduced cutout patches. Finally, the relative matching scores and values are fed to the *decoder* to generate the reconstructed image with cutout prediction and a tag map. During inference stage, the values are generated using previously predicted object segmentation masks, and the decoder yields object segmentation mask along with the tags of the current frame.

3.1 Architecture

Here, we elaborate the preliminaries of our network presented in Figure 2 and Figure 3. Using a ResNet-18 [15] backbone network Enc_{cur}, we encode the current frame I_t into current frame embedding or query Q_t. Next, the past frames I_{t-1}...I_{t-7} are encoded by Enc_{key} to generate keys K_{t-1}...K_{t-7}. These keys are concatenated to form a comprehensive key $\boldsymbol{K_t}$. Using the query and the key, attention is computed, which is used to determine the strength of the correspondence between pixels from the current and the past frames. During training, past frames introduced with cutouts I'_{t-1}...I'_{t-7} are passed through Enc_{val}. The resultant generated values V_{t-1}...V_{t-7} (collectively termed as $\boldsymbol{V_t}$) are then combined with the query and the key. We utilize this resultant representation as

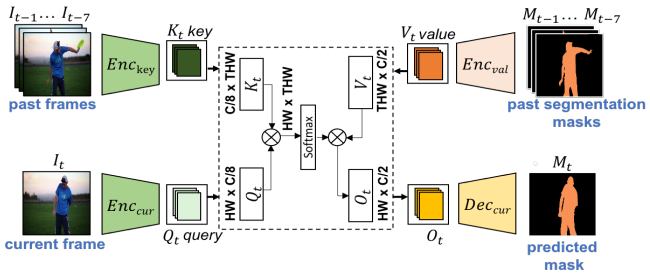

Figure 3: *Inference setup:* During testing phase, the value V_t is computed using previous segmentation masks (shown on the top right). The decoder generates object segmentation mask M_t as output. Here, V_t is generated by repeating each segmentation mask across 3 channels, and M_t is resultant single channel output by averaging the 3 channel output from the decoder normalised to range [-1, 1] that is further thresholded at 0.

input to the decoder Dec_{cur}, which yields the reconstructed image with cutout I_t^{pred} and tags P_t.

The model comprises ResNet-18 as the backbone network for current frame encoder Enc_{cur}, past frames encoder Enc_{key} as well as value encoder Enc_{val}. The base features are computed using stage-4 (res4) of the ResNet-18 model. For each input frame I_t, we have a triplet (Q_t, $\boldsymbol{K_t}$, $\boldsymbol{V_t}$) referring to Query, Key, and Value. During training, reconstruction of the cutout-based current frame (I_t^{pred}) is accomplished by combining pixels from the current frame (I_t), with pixels of past frames through attention.

To implement cutout, we apply a fixed-size zero mask to a random location in the frame. The selected random location for the cutout is retained for each image within a 10-frame clip passed through Enc_{val}, as shown in Figure 2. In addition, we apply a cutout size constrain such that at least 50% of the image remains unmodified. Concurrently, we generate multi-scale feature embeddings for one of the random past frames. This helps in dealing with multiple object sizes and finer deals, thereby enhancing the robustness of the method.

During inference, however, as illustrated in Figure 3, the approach focuses on generating object segmentation mask M_t for time frame t (current frame). While the network is trained on $\boldsymbol{V_t}$ comprising 3-channel cutout-based RGB frames, we generate 3-channel $\boldsymbol{V_t}$ from 1-channel segmentation masks M_{t-1}...M_{t-7} during inference by stacking each object mask 3 times. Also, during training, the resultant output $\boldsymbol{O_t}$ is a cutout-based reconstructed RGB frame, therefore inference involves computing resultant 1-channel segmentation output M_t by averaging 3-channel output from the decoder Dec_{cur} normalized to the range [-1, 1] and further thresholded at 0. Additionally, we do not use the tags generated during inference.

3.2 Proposed Loss Formulation

To train our network, we introduce two new losses, namely self-supervised cutout-based reconstruction loss and tagging loss, detailed below:

$$L_{overall} = L_{c\_reconstruction} + \lambda L_{c\_tagging}. \tag{1}$$

The reconstruction loss with cutout ensures that the model accounts for the less significant features within the frames as much as it focuses on the salient features. This better equips the VOS model with occlusion-based spatio-temporal discontinuities that it would encounter during inference. In addition, the self-supervised tagging loss enforces the separation of the object from the background to boost the segmentation performance. We use a combination of cutout-based reconstruction loss and λ weighted self-supervised tagging loss to train our network for segmentation (equally weighted losses give us the best results).

Reconstruction Loss with Cutout: The objective $L_{c\_reconstruction}$ to distinguish between the reconstructed frame I_t^{pred} and input frame I_t (we are dropping subscript t below for convenience), is defined in terms of Huber Loss as follows:

$$L_{c\_reconstruction} = \frac{1}{N}\sum_{j=1}^{N} z_j, \tag{2}$$

$$\text{where } z_j = \begin{cases} 0.5(I_j^{pred} - I_j)^2 & if\ |I_j^{pred} - I_j| < 1 \\ |I_j^{pred} - I_j| - 0.5 & otherwise \end{cases} \tag{3}$$

Here, N corresponds to total number of pixels in the image, and we assume pixel values in I and I^{pred} are normalized between -1 and 1.

Self-Supervised Cutout-Based Tagging Loss: We introduce the self-supervised cutout-based tagging loss that comprises a cutout pixel pull loss, L_{cp}, and cutout pixel-to-reconstructed image pixel push loss, L_{rp}, for the separation of pixels in the VOS task. Suppose, h_w is the predicted tag (or the regressed value, i.e. continuous values between 0 and 1) for a given w^{th} random pixel in the cutout region or the reconstructed image region, then let us define $h_W{}'$, that is the mean of tags for the group of W random pixels as:

$$h_W{}' = \frac{1}{W}\sum_{w=1}^{W} h_w. \tag{4}$$

In order to define L_{cp}, we only work with randomly selected subset of cutout pixels, say m where $m = 1, ...M$. Here, h_m corresponds to predicted tag for m^{th} cutout pixel, while $h_M^{'}$ refers to mean of tags of M cutout pixels. Formally, we define L_{cp} below which pulls the tags of all cutout pixels closer as:

$$L_{cp} = \frac{1}{M}\sum_{m=1}^{M} (h_m - h_M{}')^2. \tag{5}$$

In addition to pulling the tags of cutout pixels together, we also try to push apart the cutout pixels from the reconstructed image pixels. We introduce a margin G to provide a permissible gap on the difference in the embedding space of cutout pixels C and reconstructed image pixels B. Given the mean of cutout pixel tags $h_C^{'}$ and

Method	Backbone	Dataset (Size)	$J\&F$	J_{mean}	F_{mean}
Unsupervised					
Vid. Color [48]	ResNet-18	Kinetics (800 hrs)	34.0	34.6	32.7
CycleTime [51]	ResNet-50	VLOG (344 hrs)	48.7	46.4	50.0
CorrFlow [22]	ResNet-18	OxUvA (14 hrs)	50.3	48.4	52.2
UVC [24]	ResNet-18	Kinetics (800 hrs)	59.5	57.7	61.3
MAST [21]	ResNet-18	YT-VOS (5.58 hrs)	65.5	63.3	67.6
CT-VOS (Ours)	ResNet-18	YT-VOS (5.58 hrs)	**68.2**	**67.1**	**69.2**
STC [17]	ResNet-18	Kinetics (800 hrs)	68.3	65.5	71.0
CT-VOS (Ours)	ResNet-18	Kinetics (800 hrs)	**69.8**	**68.3**	**71.3**
DINO [3]	ViT [8]	ImageNet [39]	71.4	67.9	74.9
CT-VOS (Ours)	ResNet-50	Kinetics (800 hrs)	**72.6**	**69.7**	**75.4**
Supervised					
OSMN [57]	VGG-16	ICD (227k)	54.8	52.5	57.1
SiamMask [50]	ResNet-50	IVCY (2.7M)	56.4	54.3	58.5
OSVOS[2]	VGG-16	ID (10k)	60.3	56.6	63.9
OnAVOS [46]	ResNet-38	ICPD (517k)	65.4	61.6	69.1
OSVOS-S [28]	VGG-16	IPD (17k)	68.0	64.7	71.3
FEELVOS [44]	Xception-65	ICDY (663k)	71.5	69.1	74.0
PReMVOS [27]	ResNet-101	ICDPM (527k)	77.8	73.9	81.8
STM [33]	ResNet-50	IDY (164k)	81.8	79.2	84.3
SST[10]	ResNet-101	IDY (164k)	82.5	79.9	85.1
RMNet[53]	ResNet-50	IDY (164k)	83.5	81.0	86.0
LCM[16]	ResNet-50	IDY (164k)	83.5	80.5	86.5

Table 1: State-of-the-art comparison on DAVIS-2017 validation set. Here, reference dataset notations are: I=ImageNet, V=ImageNet-VID, C=COCO, D=DAVIS, M=Mapillary, P=PASCAL-VOC, Y=YouTube-VOS.

Method	G (%)	J (%)		F (%)	
		Seen	Unseen	Seen	Unseen
Unsupervised					
Vid. Color [48]	38.9	43.1	36.6	38.6	37.4
CorrFlow [22]	46.6	50.6	43.8	46.6	45.6
MAST [21]	64.2	63.9	60.3	64.9	67.7
CT-VOS	**67.1**	**67.3**	**66.1**	**68.4**	**66.5**
Supervised					
OSMN [57]	51.2	60.0	40.6	60.1	44.0
MaskTrack [34]	53.1	59.9	45.0	59.5	47.9
RGMP [32]	53.8	59.5	45.2	–	–
OnAVOS [46]	55.2	60.1	46.6	62.7	51.4
RVOS [43]	56.8	63.6	45.5	67.2	51.0
OSVOS [2]	58.8	59.8	54.2	60.5	60.7
S2S [54]	64.4	71.0	55.5	70.0	61.2
PReMVOS [27]	66.9	71.4	56.5	75.9	63.7
AGSS-VOS [25]	71.3	71.3	65.5	75.2	73.1
STM [33]	79.4	79.7	72.8	84.2	80.9
RMNet[53]	81.5	82.1	75.7	85.7	82.4
SST[10]	81.7	81.2	76.0	–	–
LCM[16]	82.0	82.2	75.7	86.7	83.4

Table 2: State-of-the-art comparison on Youtube-VOS validation set.

the mean of reconstructed image pixel tags $h_B^{'}$, the complementary margin-based penalty loss L_{rp} is given by:

$$L_{rp} = max(0, G - ||h_B^{'} - h_C^{'}||). \quad (6)$$

The self-supervised cutout-based tagging loss $L_{c\_tagging}$ that helps with separation of cutout pixels and reconstructed image pixels is defined as:

$$L_{c\_tagging} = L_{cp} + L_{rp}. \quad (7)$$

4 EXPERIMENTS

Datasets: We evaluate our approach on two VOS benchmarks: DAVIS-2017 [35] and Youtube-VOS [55]. DAVIS-2017 consists of 120 videos with 60 training, 30 validation, and 30 testing sequences. Youtube-VOS comprises 4,453 annotated videos of 91 object classes.
Training: The backbone network constitutes the ResNet-18 module and additional layers that are randomly initialized. We use random crops as well as spatial and temporal flips to augment the training data. Next, the generated single clip of 8 frames is split into past frames (initial 7 frames) and the current frame (8^{th} frame). In addition, we have 2 zoomed-in frames for one of the randomly chosen past frames, resulting in overall 10 frames per batch in a given epoch. The objective function used to optimize the network is discussed in detail in Section 3.2. For fair comparison with existing methods, we use the same training strategy as the previous self-supervised VOS works. We present the quantitative results on DAVIS-2017 validation set using backbone networks trained only on datasets mentioned under the 'Dataset' column in Table 1, and the model used to report results on YouTube-VOS validation (Table 2) is trained only using the YouTube-VOS. Our method converges on the Youtube-VOS dataset in around 400 epochs. Additionally, the model is trained using a learning rate of 0.0001 and Adam Optimizer on a Nvidia V100 GPU.
Inference: Figure 3 summarizes the testing stage. Similar to the training process, we process 10 frames at-a-time during inference. Also, during inference, similar to training phase, our model generates two outputs: 3-channel output and 1-channel of tags. Tags are primarily used for enforcing object-background separation during training and not used for mask generation during inference, which is handled by a dedicated 3-channel output (2^{nd}-row Figure 5). The predicted segmentation mask (final mask as shown in Figure 5) is determined by simply averaging the generated labels from the 3-channel output. The final segmentation generated for each current frame is, then, used as input for the subsequent clip.
Evaluation Metrics: We use the following metrics to evaluate the predicted multi-object video segmentation masks in comparison to its ground truth:

- Region similarity J: Defined by the intersection-over-union between the predicted segmentation and ground-truth mask. It provides a measure of the mislabeled pixels.

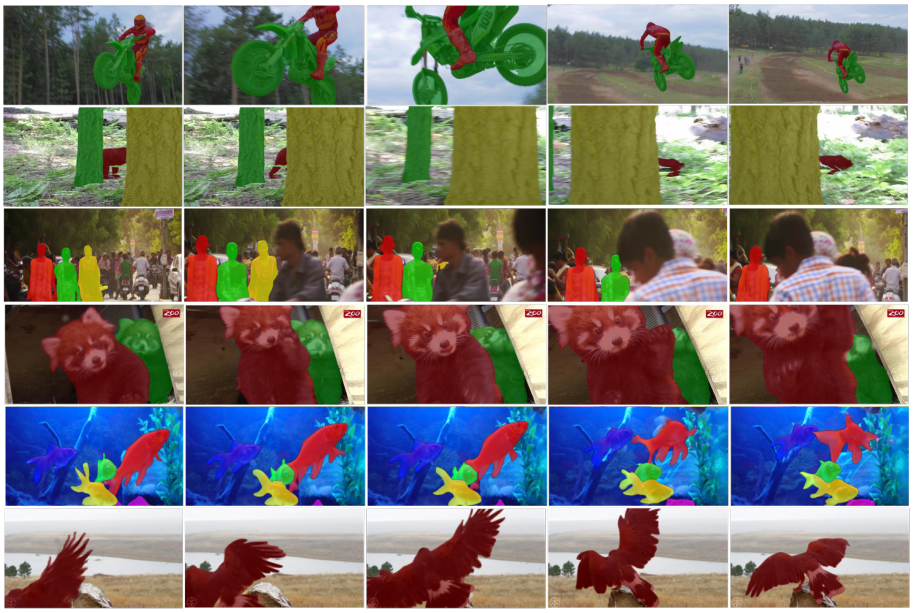

Figure 4: Qualitative results of our method on DAVIS-2017 (Rows 1, 3, 5) and Youtube-VOS (Rows 2, 4, 6). The first two rows depict the ability of the model to effectively handle visual discontinuities, namely occlusion; the next two rows illustrate that our model deals well with separating objects from a background even with highly similar distractor objects; the later rows demonstrate the model's competency with generating fine-grained segmentation details for large as well as small objects.

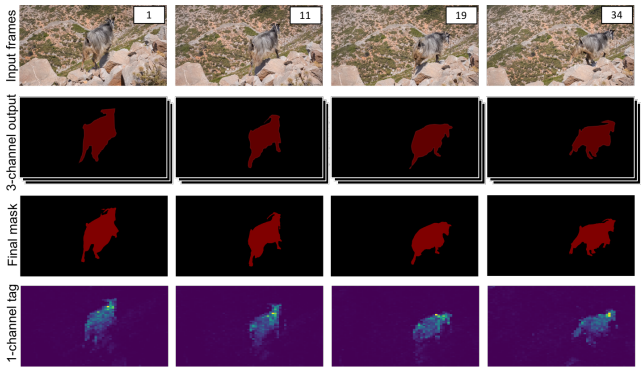

Figure 5: Decoder output visualizations during inference

- Contour precision F: Measures the contour-based precision and recall between the contour points. It is an indicator of precision of the segmentation boundaries.
- Overall score G: Average score of J and F measures.

4.1 State-of-the-art Comparison

Table 1 presents our quantitative results on DAVIS-2017 validation set. Here, we observe that proposed method outperforms existing published self-supervised work on VOS. Similarly, the results on YouTube-VOS validation set in Table 2 further affirm its ability to generate compelling segmentations. We, also, visualize the results on DAVIS-2017 and YouTube-VOS in Figure 4. Furthermore, Figure 6 highlights the improvements in segmentation that our work exhibits on DAVIS-2017 over existing self-supervised VOS methods.

Method	$J\&F$	J_{mean}	F_{mean}
Reconstruction Loss W/O Cutout	59.7	58.4	60.9
Reconstruction Loss W Cutout	63.9	63.6	64.2
+ Tagging Loss	66.3	65.9	66.7
+ Zoom-in Module	**68.2**	**67.1**	**69.2**

Table 3: Ablation when components are added sequentially on DAVIS-2017 validation set.

Method	$J\&F$	J_{mean}	F_{mean}
Circle	67.1	65.9	68.2
Scalene Triangle	67.3	66.0	68.5
Rectangle	67.9	66.7	69.1
Square	**68.2**	**67.1**	**69.2**

Table 4: Impact of varying cutout shapes on DAVIS-2017 validation set.

4.2 Ablation Study

We demonstrate the effectiveness of individual model components by adding the components sequentially. Table 3 summarizes the experiments performed on the DAVIS-2017 dataset with our baseline model using ResNet-18 backbone. In addition, Figure 7 illustrates the significance of each proposed component based on the qualitative analysis performed on DAVIS-2017.

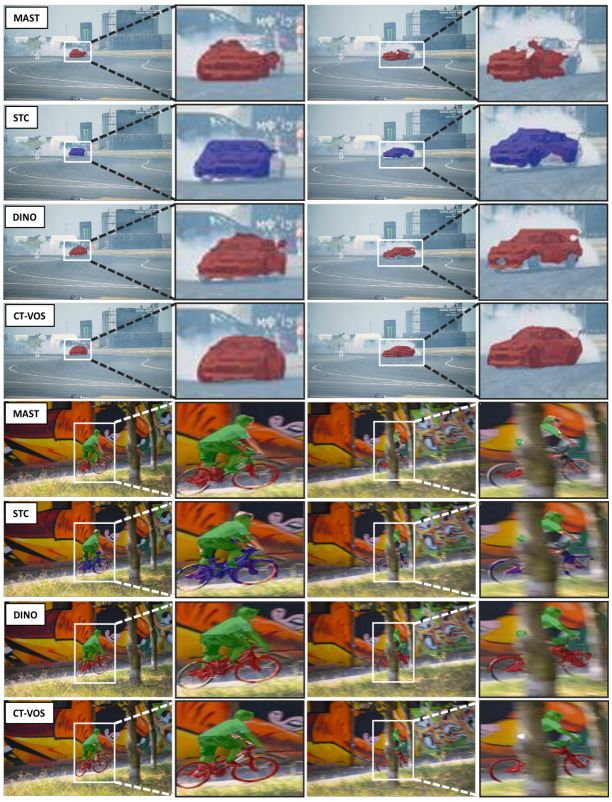

Figure 6: Qualitative results on DAVIS-2017 for comparison of our method (Rows 4, 8) against existing self-supervised VOS approaches, namely MAST [21] (Rows 1, 5), STC [17] (Rows 2, 6) and DINO [3] (Rows 3, 7). Row 4: Ability to separate objects from highly similar surrounding distractor elements. Row 8: Generation of fine-grained segmentation details and competency to deal with occlusion.

Method	$J\&F$	J_{mean}	F_{mean}
L_{cp}	65.6	66.8	64.4
L_{rp}	66.7	65.8	67.5
L_{cp+rp}	**68.2**	**67.1**	**69.2**

Table 5: The role of pull and push components in cutout-based tagging loss.

Method	$J\&F$	J_{mean}	F_{mean}
BCE Loss	65.9	66.2	65.5
Tagging Loss	**68.2**	**67.1**	**69.2**

Table 6: Ablation for binary cross-entropy loss v/s tagging loss.

Reconstruction Loss With Cutout: To investigate the influence of standard colorizing loss on the overall system design, we create a base model and analyze the resulting output (see Table 3). We introduce the LAB color palette to leverage the decorrelated color space, and augment the data using random crops and spatio-temporal flips in the baseline network. The qualitative results generated by this model with conventional colorizing loss exhibits significantly deteriorated object segmentation as seen in Figure 7(a). During

Method	$J\&F$	J_{mean}	F_{mean}
1	**68.2**	**67.1**	**69.2**
3	67.7	66.5	68.9
5	67.6	66.3	68.9

Table 7: The effect of introducing zoom-in module across multiple random past frames.

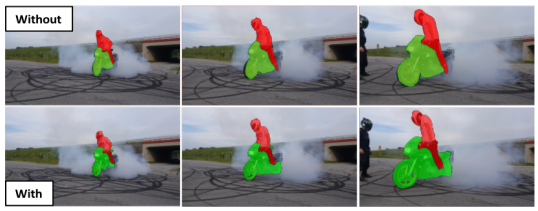

(a) Cutout-based reconstruction

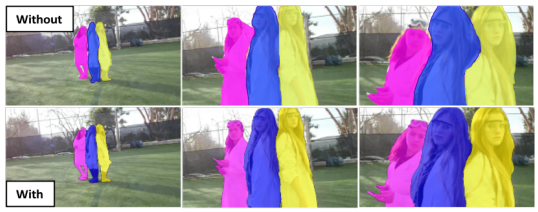

(b) Tagging loss

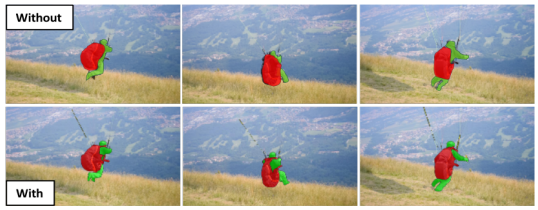

(c) Zoom-in scheme

Figure 7: Our qualitative results depicting the impact of each component, on DAVIS-2017, suggest that (a) Introducing cutout-based reconstruction improves model's ability to perceive spatio-temporal discontinuities (occlusion in our case). The rear-end of motorbike that is partially occluded is properly segmented by our model using cutouts. (b) Tagging loss helps generate accurate segmentation masks for the left most person, despite the headgear blending with the surrounding pixels, thereby validating its foreground-background decoupling capabilities. (c) Fine details of paragliding backpack are captured by our zoom-in scheme.

training, introducing cutout-based reconstruction of the images forces the model to concurrently focus on both salient as well as less salient features within the frames. Cutouts simulate occlusion-based scenarios that the model is likely to be subject to during the testing phase. It, therefore, inherently improves the generated object segmentations. Additionally, detailed analysis about shapes (refer Table 4) and sizes (refer to Table 3 from the supplementary material) of cutouts make it evident that the shape variations have inconspicuous effects on the overall performance, compared to change in the size of the cutout. The disproportionately large size of the cutout is associated with significant loss of context.

Self-supervised Cutout-Based Tagging Loss: Here, we evaluate the effectiveness of the self-supervised tagging loss in our model. Adding the self-supervised tagging loss improves the overall segmentation score of the network by ∼2% as depicted in Table 3. In Table 5, we test the model performance by introducing each component of the loss. Based on the analysis of qualitative results we notice that eliminating L_{cp} causes segmentation of an individual object instance to separate into smaller disjoint clumps, while L_{rp} plays a significant role in minimizing the background pixels overlapping foreground pixels of objects around edges. Here, L_{cp} serves as a pulling force to bring together all the pixels associated with the background, while L_{rp} pushes apart object-background pixels in close vicinity that are not related each other. Overall the tagging loss is a clustering/margin maximization-based objective. For a comprehensive ablation study, we apply binary cross-entropy loss instead of tagging loss and compare the results in Table 6. We train the model using binary cross-entropy by assigning the cutout pixels as label 0 and the rest as 1. The quantitative results validate the ability of tagging loss to improve model performance by introducing intricate foreground-background separation.

Zoom-in Views: In the final ablation study, we test the importance of zoom-in views in the network. We find that the zoom-in views capture the finer structural information and thereby promotes the prediction of finer details for small objects. Table 3 shows the impact of the zoom-in views on the quantitative results, and we see an increase of ∼2% in the overall performance. Introducing the zoom-in across multiple randomly selected past frames (see Table 7), however, fails to improve the resulting output. Since the zoom-in component focuses on exploiting the spatial information, adding it across one of the single past frame or multiple past frames improves the model outcomes by a similar value (refer to Figure 8). The proposed zoom-in structure essentially forces the model to find clean signal from multi-scale correspondence, thereby enhancing its robustness to determining correlation.

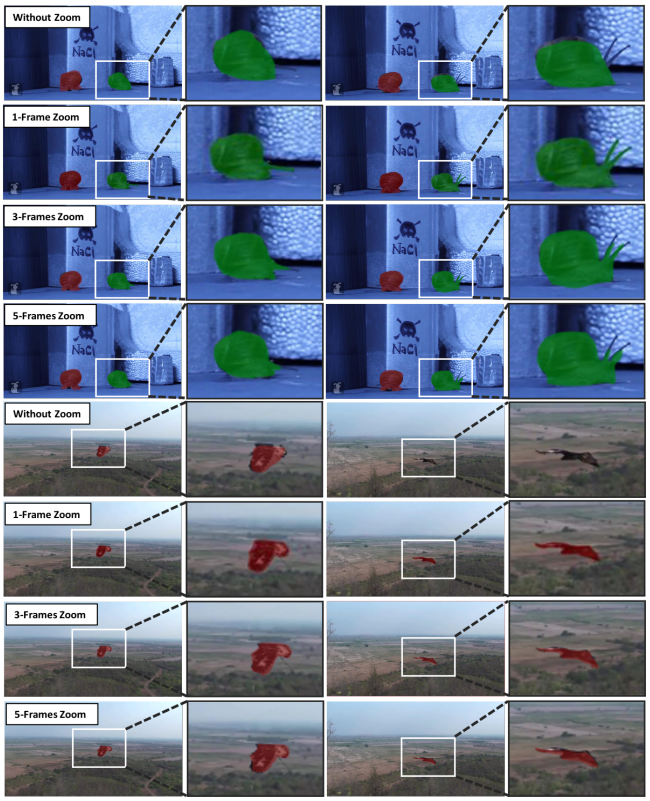

Figure 8: Qualitative results displaying the ability of zoom-in scheme to capture fine-grained segmentation details (for quantitative results refer to Table 3). In addition, we analyze the impact of introducing zoom-in module across multiple random past frames (for quantitative results refer to Table Table 7). Row 1, 2, 3, 4: Captured tentacles of the snail. Row 5, 6, 7, 8: Segmentation mask predicted for the bird's flight. Here, from the mentioned observations, it is evident that introducing the zoom-in scheme captures the finer object details, however since this component focuses on the spatial context, adding it across a single past frame or multiple past frames improves the segmentation results by a similar value.

5 CONCLUSIONS

In this work, we have proposed a self-supervised video segmentation network, which exhibits improved performance. These capabilities are driven by the self-supervised cutout-based prediction and tagging loss that ensures separation of foreground-background pixels. Additionally, the zoom-in views helps by retaining the elaborate details of objects, thereby providing the context needed for segmenting smaller objects. The overall quantitative results provide the measure of the effectiveness of the network, while the ablation studies highlight the distinct contributions of each module. Our system transforms the general reconstruction-based self-supervised approach for VOS, and has the potential to be extended to more challenging segmentation and tracking tasks.

REFERENCES

[1] Thomas Brox and Jitendra Malik. 2010. Object Segmentation by Long Term Analysis of Point Trajectories. In *Proceedings of the European Conference on Computer Vision*. Springer Berlin Heidelberg, Berlin, Heidelberg, 282–295.

[2] Sergi Caelles, Kevis-Kokitsi Maninis, Jordi Pont-Tuset, Laura Leal-Taixé, Daniel Cremers, and Luc Van Gool. 2017. One-Shot Video Object Segmentation. In *Proceedings of the IEEE/CVF Conference on Computer Vision and Pattern Recognition*.

[3] Mathilde Caron, Hugo Touvron, Ishan Misra, Hervé Jégou, Julien Mairal, Piotr Bojanowski, and Armand Joulin. 2021. Emerging Properties in Self-Supervised Vision Transformers. In *Proceedings of the IEEE/CVF International Conference on Computer Vision*. 9650–9660.

[4] Yuhua Chen, Jordi Pont-Tuset, Alberto Montes, and Luc Van Gool. 2018. Blazingly Fast Video Object Segmentation With Pixel-Wise Metric Learning.. In *Proceedings*

of the IEEE/CVF Conference on Computer Vision and Pattern Recognition. IEEE Computer Society, 1189–1198.

[5] Jia Deng, Wei Dong, Richard Socher, Li-Jia Li, Kai Li, and Li Fei-Fei. 2009. Imagenet: A large-scale hierarchical image database. In *Proceedings of the IEEE/CVF Conference on Computer Vision and Pattern Recognition*. Ieee, 248–255.

[6] Carl Doersch, Abhinav Gupta, and Alexei A Efros. 2015. Unsupervised visual representation learning by context prediction. In *Proceedings of the IEEE/CVF International Conference on Computer Vision*. 1422–1430.

[7] Nanqing Dong and Eric P Xing. 2018. Few-Shot Semantic Segmentation with Prototype Learning.. In *British Machine Vision Conference*, Vol. 3.

[8] Alexey Dosovitskiy, Lucas Beyer, Alexander Kolesnikov, Dirk Weissenborn, Xiaohua Zhai, Thomas Unterthiner, Mostafa Dehghani, Matthias Minderer, Georg Heigold, Sylvain Gelly, et al. 2020. An image is worth 16x16 words: Transformers for image recognition at scale. *arXiv preprint arXiv:2010.11929* (2020).

[9] Kevin Duarte, Yogesh S. Rawat, and Mubarak Shah. 2019. CapsuleVOS: Semi-Supervised Video Object Segmentation Using Capsule Routing. In *Proceedings of the IEEE/CVF International Conference on Computer Vision*.

[10] Brendan Duke, Abdalla Ahmed, Christian Wolf, Parham Aarabi, and Graham W Taylor. 2021. Sstvos: Sparse spatiotemporal transformers for video object segmentation. In *Proceedings of the IEEE/CVF Conference on Computer Vision and Pattern Recognition*. 5912–5921.

[11] Mark Everingham, Luc Van Gool, Christopher KI Williams, John Winn, and Andrew Zisserman. 2010. The pascal visual object classes (voc) challenge. *International Journal of Computer Vision* 88, 2 (2010), 303–338.

[12] Alon Faktor and Michal Irani. 2014. Video Segmentation by Non-Local Consensus voting. In *British Machine Vision Conference*. BMVA Press.

[13] Tengda Han, Weidi Xie, and Andrew Zisserman. 2019. Video representation learning by dense predictive coding. In *Proceedings of the IEEE/CVF International Conference on Computer Vision Workshops*. 0–0.

[14] K. He, G. Gkioxari, P. Dollár, and R. Girshick. 2017. Mask R-CNN. In *Proceedings of the IEEE/CVF International Conference on Computer Vision*. 2980–2988.

[15] Kaiming He, Xiangyu Zhang, Shaoqing Ren, and Jian Sun. 2016. Deep residual learning for image recognition. In *Proceedings of the IEEE/CVF Conference on Computer Vision and Pattern Recognition*. 770–778.

[16] Li Hu, Peng Zhang, Bang Zhang, Pan Pan, Yinghui Xu, and Rong Jin. 2021. Learning Position and Target Consistency for Memory-based Video Object Segmentation. In *Proceedings of the IEEE/CVF Conference on Computer Vision and Pattern Recognition*. 4144–4154.

[17] Allan Jabri, Andrew Owens, and Alexei Efros. 2020. Space-Time Correspondence as a Contrastive Random Walk. In *Conference on Neural Information Processing Systems*, Vol. 33. Curran Associates, Inc.

[18] Suyog Dutt Jain and Kristen Grauman. 2014. Supervoxel-Consistent Foreground Propagation in Video. In *Proceedings of the European Conference on Computer Vision*, David Fleet, Tomas Pajdla, Bernt Schiele, and Tinne Tuytelaars (Eds.). Springer International Publishing, Cham, 656–671.

[19] Dahun Kim, Donghyeon Cho, and In So Kweon. 2019. Self-supervised video representation learning with space-time cubic puzzles. In *Proceedings of the AAAI Conference on Artificial Intelligence*, Vol. 33. 8545–8552.

[20] Nikos Komodakis and Spyros Gidaris. 2018. Unsupervised representation learning by predicting image rotations. In *International Conference on Learning Representations*.

[21] Zihang Lai, Erika Lu, and Weidi Xie. 2020. MAST: A memory-augmented self-supervised tracker. In *Proceedings of the IEEE/CVF Conference on Computer Vision and Pattern Recognition*. 6479–6488.

[22] Zihang Lai and Weidi Xie. 2019. Self-supervised learning for video correspondence flow. *arXiv preprint arXiv:1905.00875* (2019).

[23] Xiaoxiao Li and Chen Change Loy. 2018. Video object segmentation with joint re-identification and attention-aware mask propagation. In *Proceedings of the European Conference on Computer Vision*. 90–105.

[24] Xueting Li, Sifei Liu, Shalini De Mello, Xiaolong Wang, Jan Kautz, and Ming-Hsuan Yang. 2019. Joint-task self-supervised learning for temporal correspondence. *arXiv preprint arXiv:1909.11895* (2019).

[25] Huaijia Lin, Xiaojuan Qi, and Jiaya Jia. 2019. AGSS-VOS: Attention Guided Single-Shot Video Object Segmentation. In *Proceedings of the IEEE/CVF International Conference on Computer Vision*.

[26] Tsung-Yi Lin, Michael Maire, Serge Belongie, James Hays, Pietro Perona, Deva Ramanan, Piotr Dollár, and C Lawrence Zitnick. 2014. Microsoft coco: Common objects in context. In *Proceedings of the European Conference on Computer Vision*. Springer, 740–755.

[27] Jonathon Luiten, Paul Voigtlaender, and Bastian Leibe. 2018. PReMVOS: Proposal-generation, Refinement and Merging for Video Object Segmentation. In *Asian Conference on Computer Vision*.

[28] K-K Maninis, Sergi Caelles, Yuhua Chen, Jordi Pont-Tuset, Laura Leal-Taixé, Daniel Cremers, and Luc Van Gool. 2018. Video object segmentation without temporal information. *IEEE transactions on Pattern Analysis and Machine Intelligence* 41, 6 (2018), 1515–1530.

[29] Ishan Misra, C Lawrence Zitnick, and Martial Hebert. 2016. Shuffle and learn: unsupervised learning using temporal order verification. In *Proceedings of the European Conference on Computer Vision*. Springer, 527–544.

[30] N.S. Nagaraja, F.R. Schmidt, and T. Brox. 2015. Video Segmentation with Just a Few Strokes. In *Proceedings of the IEEE/CVF International Conference on Computer Vision*.

[31] Mehdi Noroozi and Paolo Favaro. 2016. Unsupervised learning of visual representations by solving jigsaw puzzles. In *Proceedings of the European Conference on Computer Vision*. Springer, 69–84.

[32] Seoung Wug Oh, Joon-Young Lee, Kalyan Sunkavalli, and Seon Joo Kim. 2018. Fast Video Object Segmentation by Reference-Guided Mask Propagation. In *Proceedings of the IEEE/CVF Conference on Computer Vision and Pattern Recognition*.

[33] Seoung Wug Oh, Joon-Young Lee, Ning Xu, and Seon Joo Kim. 2019. Video object segmentation using space-time memory networks. In *Proceedings of the IEEE/CVF International Conference on Computer Vision*. 9226–9235.

[34] F. Perazzi, A. Khoreva, R. Benenson, B. Schiele, and A. Sorkine-Hornung. 2017. Learning Video Object Segmentation from Static Images. In *Proceedings of the IEEE/CVF Conference on Computer Vision and Pattern Recognition*. 3491–3500.

[35] Jordi Pont-Tuset, Federico Perazzi, Sergi Caelles, Pablo Arbeláez, Alex Sorkine-Hornung, and Luc Van Gool. 2017. The 2017 davis challenge on video object segmentation. *arXiv preprint arXiv:1704.00675* (2017).

[36] Kate Rakelly, Evan Shelhamer, Trevor Darrell, Alyosha Efros, and Sergey Levine. 2018. Conditional networks for few-shot semantic segmentation. *International Conference on Learning Representations Workshops* (2018).

[37] Hasnain Raza, Mahdyar Ravanbakhsh, Tassilo Klein, and Moin Nabi. 2019. Weakly supervised one shot segmentation. In *Proceedings of the IEEE/CVF International Conference on Computer Vision Workshops*.

[38] Shaoqing Ren, Kaiming He, Ross Girshick, and Jian Sun. 2015. Faster R-CNN: Towards Real-Time Object Detection with Region Proposal Networks. In *Conference on Neural Information Processing Systems*. Curran Associates, Inc., 91–99.

[39] Olga Russakovsky, Jia Deng, Hao Su, Jonathan Krause, Sanjeev Satheesh, Sean Ma, Zhiheng Huang, Andrej Karpathy, Aditya Khosla, Michael Bernstein, et al. 2015. Imagenet large scale visual recognition challenge. *International journal of computer vision* 115, 3 (2015), 211–252.

[40] Amirreza Shaban, Shray Bansal, Zhen Liu, Irfan Essa, and Byron Boots. 2017. One-shot learning for semantic segmentation. *arXiv preprint arXiv:1709.03410* (2017).

[41] Mennatullah Siam, Boris N Oreshkin, and Martin Jagersand. 2019. Amp: Adaptive masked proxies for few-shot segmentation. In *Proceedings of the IEEE/CVF International Conference on Computer Vision*. 5249–5258.

[42] P. Tokmakov, K. Alahari, and C. Schmid. 2017. Learning Video Object Segmentation with Visual Memory. In *Proceedings of the IEEE/CVF International Conference on Computer Vision*. 4491–4500.

[43] Carles Ventura, Miriam Bellver, Andreu Girbau, Amaia Salvador, Ferran Marques, and Xavier Giro-i Nieto. 2019. Rvos: End-to-end recurrent network for video object segmentation. In *Proceedings of the IEEE/CVF Conference on Computer Vision and Pattern Recognition*. 5277–5286.

[44] Paul Voigtlaender, Yuning Chai, Florian Schroff, Hartwig Adam, Bastian Leibe, and Liang-Chieh Chen. 2019. Feelvos: Fast end-to-end embedding learning for video object segmentation. In *Proceedings of the IEEE/CVF Conference on Computer Vision and Pattern Recognition*. 9481–9490.

[45] Paul Voigtlaender, Yuning Chai, Florian Schroff, Hartwig Adam, Bastian Leibe, and Liang-Chieh Chen. 2019. FEELVOS: Fast End-to-End Embedding Learning for Video Object Segmentation. In *Proceedings of the IEEE/CVF Conference on Computer Vision and Pattern Recognition*.

[46] Paul Voigtlaender and Bastian Leibe. 2017. Online Adaptation of Convolutional Neural Networks for Video Object Segmentation. In *British Machine Vision Conference*. BMVA Press.

[47] Carl Vondrick, Hamed Pirsiavash, and Antonio Torralba. 2016. Anticipating visual representations from unlabeled video. In *Proceedings of the IEEE/CVF Conference on Computer Vision and Pattern Recognition*. 98–106.

[48] Carl Vondrick, Abhinav Shrivastava, Alireza Fathi, Sergio Guadarrama, and Kevin Murphy. 2018. Tracking emerges by colorizing videos. In *Proceedings of the European Conference on Computer Vision*. 391–408.

[49] Kaixin Wang, Jun Hao Liew, Yingtian Zou, Daquan Zhou, and Jiashi Feng. 2019. Panet: Few-shot image semantic segmentation with prototype alignment. In *Proceedings of the IEEE/CVF International Conference on Computer Vision*. 9197–9206.

[50] Qiang Wang, Li Zhang, Luca Bertinetto, Weiming Hu, and Philip HS Torr. 2019. Fast online object tracking and segmentation: A unifying approach. In *Proceedings of the IEEE/CVF Conference on Computer Vision and Pattern Recognition*. 1328–1338.

[51] Xiaolong Wang, Allan Jabri, and Alexei A Efros. 2019. Learning correspondence from the cycle-consistency of time. In *Proceedings of the IEEE/CVF Conference on Computer Vision and Pattern Recognition*. 2566–2576.

[52] Donglai Wei, Joseph J Lim, Andrew Zisserman, and William T Freeman. 2018. Learning and using the arrow of time. In *Proceedings of the IEEE/CVF Conference on Computer Vision and Pattern Recognition*. 8052–8060.

[53] Haozhe Xie, Hongxun Yao, Shangchen Zhou, Shengping Zhang, and Wenxiu Sun. 2021. Efficient Regional Memory Network for Video Object Segmentation. In

Proceedings of the IEEE/CVF Conference on Computer Vision and Pattern Recognition. 1286–1295.

[54] Ning Xu, Linjie Yang, Yuchen Fan, Jianchao Yang, Dingcheng Yue, Yuchen Liang, Brian L. Price, Scott Cohen, and Thomas S. Huang. 2018. YouTube-VOS: Sequence-to-Sequence Video Object Segmentation.. In *Proceedings of the European Conference on Computer Vision*, Vol. abs/1809.00461. 603–619.

[55] Ning Xu, Linjie Yang, Yuchen Fan, Dingcheng Yue, Yuchen Liang, Jianchao Yang, and Thomas Huang. 2018. Youtube-vos: A large-scale video object segmentation benchmark. *arXiv preprint arXiv:1809.03327* (2018).

[56] Charig Yang, Hala Lamdouar, Erika Lu, Andrew Zisserman, and Weidi Xie. 2021. Self-supervised Video Object Segmentation by Motion Grouping. *arXiv preprint arXiv:2104.07658* (2021).

[57] L. Yang, Y. Wang, X. Xiong, J. Yang, and A. K. Katsaggelos. 2018. Efficient Video Object Segmentation via Network Modulation. In *Proceedings of the IEEE/CVF Conference on Computer Vision and Pattern Recognition*. 6499–6507.

[58] Chi Zhang, Guosheng Lin, Fayao Liu, Jiushuang Guo, Qingyao Wu, and Rui Yao. 2019. Pyramid graph networks with connection attentions for region-based one-shot semantic segmentation. In *Proceedings of the IEEE/CVF International Conference on Computer Vision*. 9587–9595.

[59] Chi Zhang, Guosheng Lin, Fayao Liu, Rui Yao, and Chunhua Shen. 2019. Canet: Class-agnostic segmentation networks with iterative refinement and attentive few-shot learning. In *Proceedings of the IEEE/CVF Conference on Computer Vision and Pattern Recognition*. 5217–5226.

[60] Fangrui Zhu, Li Zhang, Yanwei Fu, Guodong Guo, and Weidi Xie. 2020. Self-supervised Video Object Segmentation. *arXiv preprint arXiv:2006.12480* (2020).